Anne DE WIT
Unité de Chimie Physique Non Linéaire,
Service de Chimie Physique et Biologie Théorique,
Faculté des Sciences,Université Libre de Bruxelles (ULB),
Campus Plaine, CP 231, 1050 Bruxelles,
Tél: +32 (0)2 650 5774, adewit@ulb.ac.be

Chemo-hydrodynamic Patterns and Instabilities

Keywords
Chemical fronts, reaction front, reaction-diffusion, convection, hydrodynamics, fingering, Rayleigh-Taylor, Marangoni, patterns

1. Introduction

Chemical reactions interplay with fluid motions in numerous situations of every day's life. As an example, flow induced spreading of chemical pollutants and their interaction with the environment is a problem of major concern in our society. Prescribing norms on the authorized concentration of chemicals in the atmosphere or in rivers depends on a good description of the concentration dependence on time and space, which in turn depends on knowledge of the chemical kinetics and on the velocity of the fluid carrying the chemical species. In the same spirit, hydrodynamic deformations of interfaces between two reactive fluids as well as flows induced by chemical reactions at the front between two initially steady fluids are frequently encountered in combustion, petroleum, chemical and pharmaceutical engineering.

There is a vast literature studying the influence of fluid flows on the transport of passive chemical species. The situation becomes more complex if the chemical reactions affect the flow properties themselves such as its density or viscosity for instance. In that case, the chemistry can be at the very origin of hydrodynamic instabilities inducing motions unexpected in non-reactive systems. As a corollary, the hydrodynamic flows can in turn affect the yield of the reactions and an interesting feedback between chemistry and hydrodynamics sets then in. Unfortunately, these situations become often very intricate because of the large number of variables involved and because several different effects (solutal vs thermal effects, density, viscosity vs surface tension effects) may come into play. Beyond classical engineering approaches dealing efficiently with such a complexity, the fundamental understanding of the dynamics of reactive fluids can benefit from the study of simpler model systems.

In this context, research in our group in the Nonlinear Physical Chemistry Unit of ULB aims at studying the coupling between chemical reactions and hydrodynamic instabilities from a fundamental theoretical (and more recently also experimental) perspective. Our goal is specifically to study simple model systems in which only one mechanism of hydrodynamic instability is at play and for which a one or two-variable model can describe the chemical reactions. To do so, we focus on chemo-hydrodynamic patterns and instabilities developing around interfaces between miscible reactive solutions and which are due to chemically driven gradients in the physical properties of the solution. In other words, we are not analyzing systems where the chemicals are merely passively advected by prescribed flows. We are rather focusing on situations where the chemistry is *actively* driving the flow or even more is at the very source of the hydrodynamic instability. This occurs if the chemical reaction is influencing the density, surface tension or viscosity of the solution across a given interface. Such interfaces exist in reactive systems either if two solutions each containing one given reactant are initially put in contact or if specific reactions coupled to diffusion generate self-sustained chemical fronts.

Autocatalytic chemical reactions in which one product of the reaction feedbacks onto its own production are examples of such specific reactive systems which can provide reaction-diffusion fronts corresponding to self-organized interfaces separating reactants and products and traveling at a constant speed. A large part of our research on chemo-hydrodynamic patterns that will be summarized below is focusing on analyzing the influence of hydrodynamic flows on such autocatalytic fronts. As such, our study of chemo-hydrodynamic patterns in autocatalytic systems participates also in the development of new research paths in nonlinear chemistry. The experimental and theoretical studies of clock reactions in batch reactors as well as of bistability, chemical oscillations and chaos in continuously stirred tank reactors have witnessed a major development since the sixties [1,2]. Numerous efforts have been invested in kinetic studies aiming at deciphering the autocatalytic and feedback processes at the heart of the complex temporal dynamics. In the eighties, the construction of open continuously fed gel reactors has allowed to add the diffusive spatial component to the problem and beautiful spatio-temporal patterns such as controlled waves, spirals and Turing patterns have then

been successively observed and studied in detail [1,2,3]. Our present work contributes to this physico-chemical approach analyzing increasing spatial complexity by adding convection on top of nonlinear chemistry and molecular diffusion. The hydrodynamically unstable autocatalytic fronts correspond in that context to a class of dissipative spatio-temporal structures developing in spatially extended systems [1].

Eventually, let us note that the research presented here is genuinely interdisciplinary in nature as it aims to understand the additional complexity that hydrodynamics brings into the field of reaction-diffusion patterns and in parallel analyzes the influence of active chemical reactions on pure hydrodynamic instabilities yielding insight into several chemical, physical or engineering applications.

Our experimental and theoretical contribution to the analysis of chemo-hydrodynamic patterns and instabilities will be presented according to the following outline. In section 2, we recall first the various hydrodynamic instabilities that will be discussed here and introduce the experimental geometries in which experiments are performed. We define also in more details the two types of reactive interfaces that will be discussed. Section 3 and 4 address the influence of density and surface tension changes across an autocatalytic traveling front before buoyancy effects on simple A+B-->C fronts are discussed in section 5. We will end up by a discussion of viscous fingering situations in section 6.

2. Reaction-driven hydrodynamic flows

Across an interface between two different miscible fluids, hydrodynamic motions can be induced if gradients in a physical property of the fluids such as density, surface tension or viscosity are present. For instance, if a denser solution lies above a lighter one in the gravity field, a Rayleigh-Taylor instability can trigger fluid motions, as the heavier fluid tends to sink while the lighter one is rising. Such a hydrodynamic instability also called "density fingering" deforms the interface into fingers of one fluid penetrating the other one [4]. When surface tension gradients are present at the interface between a liquid solution and the air, so-called Marangoni effects yield fluid motions tangential to the interface, which, by continuity, drive convection inside the bulk of the layer [5]. Eventually, if viscosity gradients are present, a hydrodynamic instability of the interface can also occur if the less viscous fluid is injected into the more viscous one which deforms the interface into fingers hence the name "viscous fingering" given to that instability [6].

Two types of geometries are typically used to study experimentally such hydrodynamic instabilities: the first one consists in a Hele-Shaw cell (two glass or Plexiglas plates separated by a thin gap width) filled with the fluids. If the gap width a of the cell is much smaller than its width L_y or length L_x (typically $a \approx 0.5$ mm or less for L_x, L_y of the order of 10 to 15 cm or more), the evolution of the fluid flow velocity $\underline{u}$ inside the cell can be described along with the incompressibility condition $\nabla \underline{u} = 0$ by Darcy's law

$$\nabla p = -\frac{\mu}{K}\underline{u} + \rho \underline{g} \qquad (1)$$

relating linearly the gradient of pressure ∇p to a buoyancy force term ρg and to the velocity $\underline{u}$ via a proportionality factor μ / K called the mobility and depending on the viscosity μ of the fluid and the permeability $K = a^2/12$ of the cell. In fact, this equation describes classically fluid flows inside porous media of permeability K so that Hele-Shaw cells are often viewed as an interesting laboratory tool to study transport processes inside porous media [6]. If the Hele-Shaw cell plates are oriented vertically in the gravity field (Fig.1), gravity points along the direction of the height of the cell. The dynamics is then genuinely two-dimensional and is easy to visualize through the transparent plates.

The second geometry consists in a Petri dish type of system i.e. a thin layer of solution lying horizontally in the gravity field in contact with air. If the solution is covered, the situation is equivalent to a Hele-Shaw cell lying horizontally with gravity pointing perpendicularly to the plates. The problem is then followed in a 2D plane consisting in a cut across the layer (see Fig.3) and the velocity of the flow obeys Stokes equation

$$\nabla p = \mu \nabla^2 \underline{u} + \rho \underline{g} \qquad (2)$$

In the problems we are interested in, one of the physical properties of the fluid varies with the concentration c_i of chemical species i. It can be the viscosity μ, the density ρ or the surface tension γ. To describe the dynamics of the system, it is then needed to couple the evolution equation for the velocity $\underline{u}$ to a reaction-diffusion-convection equation for the concentration c_i of chemical species i of the type

$$\frac{\partial c_i}{\partial t} + \underline{u} \cdot \nabla c_i = D_i \nabla^2 c_i + f(c_i) \qquad (3)$$

where $f(c_i)$ is the chemical kinetics term and D_i the diffusion coefficient. The hydrodynamic flows come then into play when an interface between solutions of different concentration and thus different physical properties is present in the Hele-Shaw cell or the Petri dish. Such an interface can be obtained either because the reaction itself creates the interface when coupled to diffusion or if two separated solutions containing each a given reactant are put in contact.

The first class of interface is the one resulting from the coupling between diffusion and specific nonlinear reactions implying autocatalytic feedbacks. It is known that this coupling is able to generate traveling fronts through which an autocatalytic species invades a given reactant such as in a combustion front [2]. As the composition of the reactant solution is different from that of the product one, hydrodynamic flows can be produced by either buoyancy or surface tension-driven effects. Let us first review now in sections 3 and 4 the chemo-hydrodynamic patterns that result from such hydrodynamic effects on autocatalytic fronts before addressing the case of the other type of interface later.

3. Buoyancy-driven instabilities of autocatalytic chemical fronts

Propagating autocatalytic fronts provide a nice model system to study chemo-hydrodynamic patterns as they genuinely create internal concentration and temperature gradients and

thus possible gradients of physical properties of the solution. Indeed, in these systems, the chemical reaction generates not only a self-organized interface between the products and the reactants when coupled to diffusion but also a density jump for instance between the solutions.

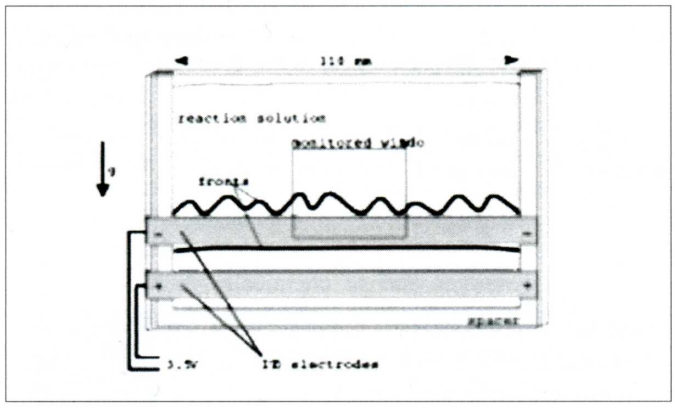

Fig.1: Sketch of a Hele-Shaw set-up oriented vertically in the gravity field in which two counter-propagating autocatalytic traveling fronts are produced when current is switched on at an electrode. If the reactants ahead of the front are heavier than the products behind it, the upward moving front is buoyantly unstable with regard to a Rayleigh-Taylor instability. The downward moving front remains planar because the density stratification is stable there.

This is due to the fact that the density of a solution is function of both composition and temperature, which naturally can vary across a traveling front. Following Pojman and Epstein who have first classified such buoyancy-driven effects in the context of autocatalytic fronts [2,7], let us discuss what dynamics can be expected. The total density of a given solution can be related to the compositional and thermal variations through the thermal α_T and the solutal α_C expansion coefficients as:

$$\rho = \rho_o + \sum_i \alpha_{ic}(c_i - c_{io}) + \alpha_T(T - T_o) \qquad (4)$$

where ρ_o is the density of the solution at room temperature T_o and concentration c_{io} of the chemical species i in the reactant solution. As a reaction proceeds there will be changes in the composition of the solution and if the reaction is exo- or endothermic it will furthermore lead to an increase or decrease of the temperature of the solution. In the case of autocatalytic fronts no endothermic reaction are known up to now so we always consider exothermic reactions increasing the temperature behind the front.

Across a front, the total density jump $\Delta\rho$ (defined as the density of the product solution minus that of the reactant solution) is the sum of a solutal and thermal contribution respectively i.e. $\Delta\rho = \Delta\rho_C + \Delta\rho_T$. Here, $\Delta\rho_T$ is always negative as the reaction is exothermic. Depending on the kinetics at hand, $\Delta\rho_c$ can on the contrary take positive or negative sign. If $\Delta\rho_c < 0$, then both solutal and thermal effects contribute to decrease the density behind the front. This is the case for instance in the redox iodate arsenous acid system well known to feature autocatalytic traveling fronts and for which the density decreases in the course of reaction because of both solutal and thermal effects [2,7,8]. In such systems, fronts *ascending* in the gravity field (Fig.2) feature an unstable density stratification of heavy reactants at room temperature above solute lighter and hotter products prone to develop a Rayleigh-Taylor instability. The ascending front hence does not remain planar but deforms into fingers induced by convective motions in the solution (Fig.2) while the descending front remains stable and planar.

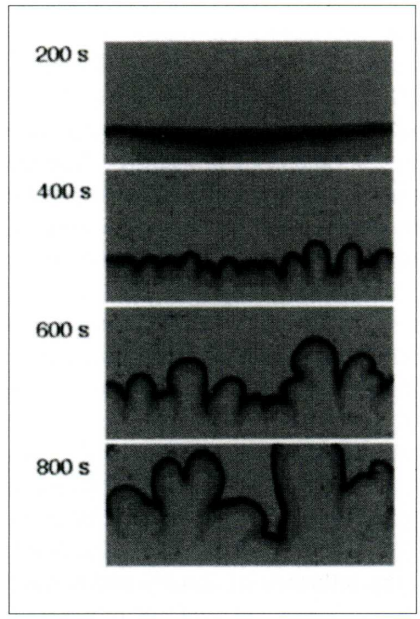

Fig.2: Experimental fingering of the iodate-arsenous acid reaction front in a vertical Hele-Shaw cell (width=43 mm) showing the time evolution of the initial pattern (courtesy M. Böckmann and S. C. Müller, Magdeburg).

If on the contrary, $\Delta\rho_c < 0$ then solutal and thermal effects are competing. In this case, the density stratification is directly unstable when the destabilizing contribution is of largest amplitude. More subtle situations come into play when the initial density stratification is stable (the stabilizing factor is of largest amplitude). The system has been shown then to be able to nevertheless destabilize because of either double-diffusive effects induced by a differential diffusion of heat and mass [9] or because of chemically driven new instabilities [10].

In the last decade, numerous theoretical and experimental studies have characterized the dynamics of such buoyantly unstable fronts in Hele-Shaw geometries (see [2,7-16] and references therein). We have contributed to this research by a theoretical approach that has given estimates of the wavelength of the pattern at onset as well as a description of the patterns in the fully developed nonlinear regime both for isothermal [8,13,14] and thermally affected fronts [9,10,15,16]. We have also analyzed influence of thermal losses through the walls of the reactor on the stability and nonlinear properties of such fronts traveling parallel to the gravity field [15].

More recently, we have also investigated what happens if such autocatalytic fronts travel in Hele-Shaw cells oriented horizontally in the gravity field or equivalently in solutions contained in a covered Petri dish [17]. In that case, the density difference between the products and reactants acts across a vertical interface, which is a situation always unstable as the lighter solution immediately starts sinking below the heavier one. In isothermal situations, the system after a given transient reaches an asymptotic dynamics in which a rotating vortex travels with the front at a speed larger than the reaction-diffusion one and deforms it in the depth of the layer. For systems where heat effects are competing with solutal ones, oscillatory convective dynamics can be evidenced in which the deformation of the front switches periodically from a tongue of

heavier fluid sinking in the lighter one towards a planar front again when the reaction takes over, this evolution cycling on and on around the traveling front.

The situation of such autocatalytic fronts traveling in horizontal solutions can be quite different if now the upper interface is not covered but open to the air.

4. Marangoni-driven instabilities of autocatalytic chemical fronts

If isothermal autocatalytic fronts are traveling horizontally in solutions open to the air in a Petri dish, gradients of concentration across the front can also trigger gradients of the surface tension γ (Fig.3) if one of the chemicals is surface active [18]. These spatial variations of the surface tension can in turn trigger Marangoni flows that will affect the spatio-temporal distribution of the concentrations in the system.

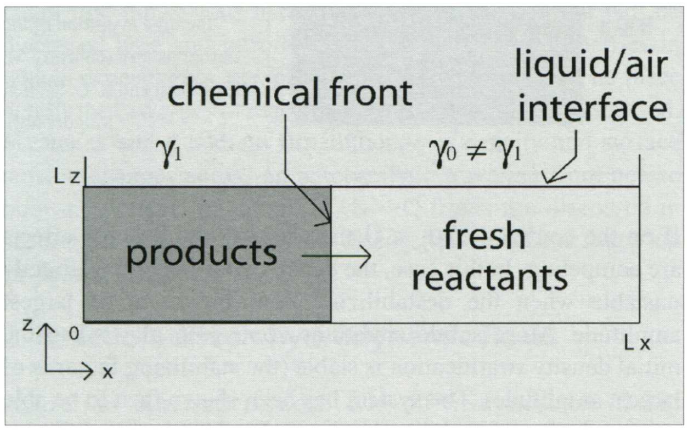

Fig.3: Sketch of a vertical cut in a Petri dish where a chemical front is traveling horizontally in a solution layer open to the air. The gradients of concentration between the reactants and the products yield gradients of surface tension γ.

To get insight into the related chemo-hydrodynamics, we have performed numerical studies of Stokes equation (2) for the flow velocity coupled to a reaction-diffusion-convection equation (3) for the concentration c of the autocatalytic product of the reaction through a boundary condition involving a Marangoni effect in absence of any buoyancy effects (constant density). Explicitly, we have that, at the upper interface between the solution and the air, the horizontal component of the fluid velocity u varies in the depth of the layer (z direction) proportionally to the gradient of concentration along the horizontal direction x i.e.:

$$\frac{\partial u}{\partial z} = -M \frac{\partial c}{\partial x} \qquad (5)$$

where M is the Marangoni number of the problem quantifying the way the surface tension varies with c i.e. $M \propto -\partial\gamma / \partial c$. The Marangoni number is positive if the surface-active species (here the product) decreases the surface tension behind the front. As a Marangoni flow is always triggered towards the zone with the highest surface tension, we have therefore that, for positive M, the flow will be triggered to the right. Starting as an initial condition from a traveling front in absence of any flow, we find numerically that surface tension gradients at the surface of the layer generate indeed acceleration of the liquid velocity towards the reactants. As the fluid is incompressible, this generates a vortex turning clockwise in the bulk of the layer. After a transient, the dynamics always asymptotes towards a front deformed by one or more vortices and traveling at a constant speed larger than the reaction-diffusion speed (Fig.4). The number of vortices, their direction of propagation, the intensity of the convection and the deformation of the concentration field can be characterized as a function of the Marangoni number, the height of the layer and the kinetics of the reaction [19-21]. These results provide a first insight into the understanding of acceleration of traveling fronts observed in open Petri dishes (see [19] and refs therein). They contribute also to a characterization of new nonlinear reaction-diffusion-convection dynamics and of chemically driven Marangoni effects. Further perspectives in that regard will be to take also into account possible dependence of Marangoni flows on thermal effects due to the exothermicity of the reaction.

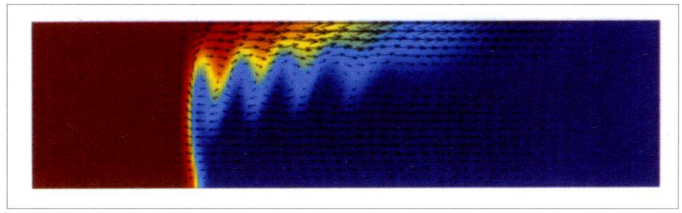

Fig.4: Marangoni-driven flow around an autocatalytic chemical front traveling in a horizontal liquid layer with a free surface on top. The arrows indicate the velocity of the fluid flow in a 2D view representing a vertical cut in the Petri dish while the colors correspond to the concentration of the autocatalytic species ranging from c=1 (red) in the product to c=0 (blue) in the reactant.

5. Buoyancy-driven deformation of simple A+B->C fronts

Another type of reaction front is encountered when two miscible solutions each containing one reactant of a simple bimolecular reaction A+B-->C are put into contact. Due to the coupling between reaction and diffusion processes, a localized reaction zone extends in time around the initial position of contact between the two solutions. The reaction front is here defined as the location where the production rate of the product C is maximum. The scalings of the propagation of this reaction-diffusion front have been thoroughly studied in the past. Theoretical studies on the diffusion-limited problem have shown that, for long times, the front position scales as a square root of time and that, for equal diffusion coefficients and initial concentrations, the reaction front is stationary i.e. remains at the initial location of contact [22]. Those theoretical works are in good agreement with convection-free experimental studies [23].

However, experiments in horizontal solutions contained between two plates yield very different results to their gel counterparts even with a very narrow gap width. This is supposed to be due to buoyancy-driven convection. As an example, experimental results by Shi and Eckert [24] are in agreement with the front position scaling of $t^{1/2}$ but there is a discrepancy between the actual front position and the theoretically predicted reaction-diffusion one. The experimental fronts have traveled much further than the predictions from the standard reaction-

diffusion model even for very thin solution layers. It seems likely that buoyancy effects have induced convection currents so that the reaction is no longer diffusion limited.

In this framework, we are performing theoretical studies to show how buoyancy-driven convection affects the problem and modifies the reaction-diffusion dynamics even for very small layer heights. By numerically integrating the two-dimensional incompressible Stokes equation (2) coupled to reaction-diffusion-convection equations (3) for the concentration of the three chemical species A, B and C, we show that the presence of convection not only deforms the reaction front in the layer (Fig.5) but also drastically alters its propagation.

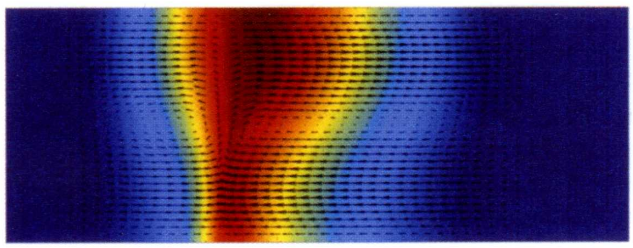

Fig.5: Numerical simulation of buoyancy-driven convection around a reaction front where the simple A+B-->C reaction takes place between two solutions containing each of the reactant separately. The arrows show the velocity of the flow superimposed on the concentration field of the product C ranging from its maximum value in red to its minimum one in blue.

We have developed analytical criteria to classify the various possible regimes for the case of equal diffusive rates with initially equal concentrations [25]. In this case, the dynamics of the front in the presence of convection can be predicted from the one-dimensional reaction-diffusion density profiles. In the case of different initial concentrations, we have shown how convection affects the reaction front dynamics, leading to its acceleration and, for some parameters, to a reversal of the propagation direction.

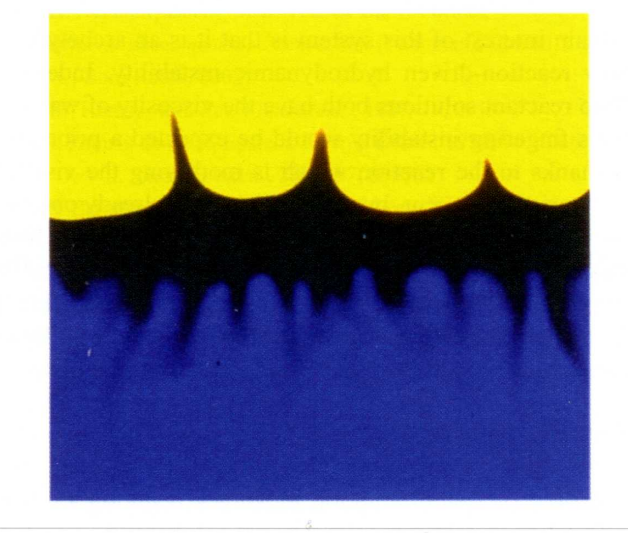

Fig.6: Buoyancy-driven deformation of an interface between a 0.01M solution of HCl (yellow) put on top of a heavier 0.01M solution of NaOH (blue) inside a Hele-Shaw cell oriented vertically in the gravity field with bromocresol green as color indicator. The field of view is 3 cm and the image is taken 5 min after contact.

Very recently, we have also started analyzing numerically and experimentally what happens if such A+B-->C fronts are developing in a Hele-Shaw cell oriented vertically in the gravity field. If the lighter solution is put on top of the heavier one, a Rayleigh-Taylor instability is setting in immediately after contact. More interesting situations have been however evidenced in some cases where the lighter solution is put on top of the heavier one [26]. Differential diffusion and density between the three species of the problem i.e. the two reactants A and B and the product C can lead to the growth of locally unfavorable density gradients or to double-diffusion instabilities [27]. As an example, Fig.6 shows the hydrodynamic deformation of the interface between a solution of HCl put on top of an equimolar solution of NaOH. Even if the acid solution is lighter than the alkaline one for the concentrations chosen, buoyancy-driven deformation of the interfacial region is observed after contact. The fact that the acid diffuses faster than the base is supposed to be at the origin of the hydrodynamic instability but more theoretical and experimental work needs to be performed to clarify such recent experimental results.

6. Viscous fingering in reactive systems

Viscous fingering is a hydrodynamic instability that occurs in a porous medium when a less viscous fluid displaces a more viscous one [6]. The interface between the two fluids is then unstable and deforms in the shape of « fingers » hence the name fingering. Such instability has been widely studied in the framework of petroleum engineering where fingering occurs when a given fluid (typically water) is injected into underground reservoirs to displace petroleum. As water is less viscous than petroleum, viscous fingering deforms the interface, which is detrimental to oil recovery as it mixes the fluids and diminishes therefore the yield of the extraction.

Viscous fingering in chromatographic columns

Viscous fingering has been recognized to also be detrimental for separation techniques in chromatographic separation of viscous samples (like typically concentrated samples of polymers or proteins in SEC – size exclusion chromatography) [28-31]. Indeed, in that case, the eluent of given viscosity displaces a miscible but more viscous sample which leads to viscous fingering of the rear interface of this sample (see Fig.7).

Such fingering contributes to the deformation and widening of the output peaks. Using numerical simulations of Darcy's law (1) coupled to an evolution equation (3) for the concentration c of a solute ruling the viscosity of the sample [30, 31], we have been able to quantify the influence of such viscous fingering on the variance of the output peaks. We show that depending on the parameters of the problem (like typically the ratio of viscosities, the length of the sample or the ratio of transverse vs axial dispersion coefficients in the chromatographic column), the widening of the peak can be increased up to 30% when fingering operates in the column for typical chromatographic conditions [31]. More recently, we have generalized this first approach to the case where the solutes in the viscous sample undergo retention on the porous matrix [32].

In parallel, model experimental systems are currently developed in our group using horizontal Hele-Shaw cells in which finite

width samples are displaced by a miscible less viscous fluid in order to quantify experimentally the influence of VF on widening of such samples (Fig.8) and test the theoretical predictions.

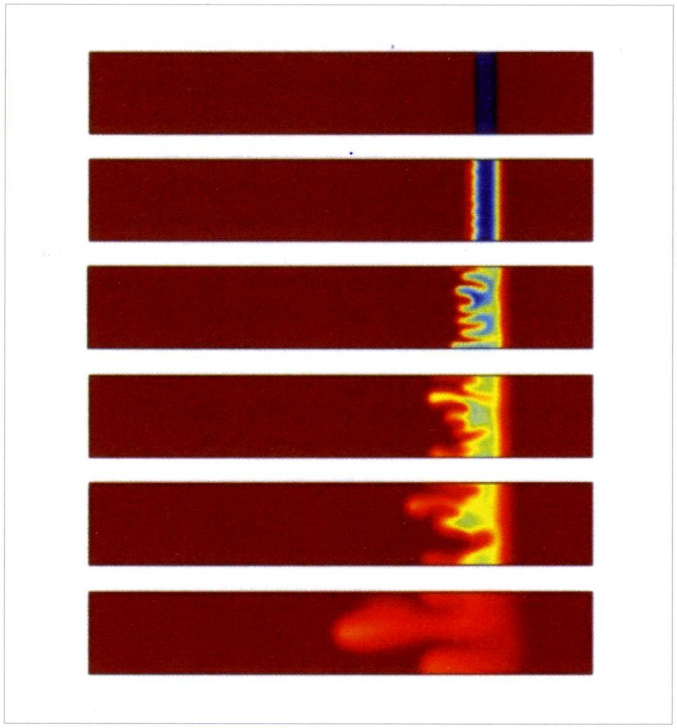

Fig.7 : Numerical simulation of viscous fingering of the rear front of a viscous sample displaced from left to right by a less viscous miscible fluid. The dynamics is shown in a frame moving with the injection speed.

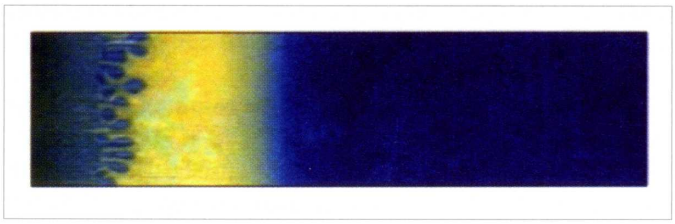

Fig.8 : Experimental view of viscous fingering of a finite sample of glycerol (yellow) displaced from left to right in a horizontal Hele-Shaw cell within less viscous water colored in blue. The frontal interface is stable while the rear interface where water displaces less viscous glycerol features a viscous fingering instability that contributes to a widening of the glycerol sample in time.

Reaction-driven viscous fingering

Recently, experiments have shown that chemical reactions can also be directly at the source of viscous fingering patterns when the viscosity of the solution changes drastically in the course of reaction [33,34]. Consider two solutions of same viscosity containing each a different reactant (say A and B) that are put in contact and react according to the simple scheme A+B--> C. A hydrodynamic viscous fingering can occur if the product C has a different viscosity than that of the reactants.

We are investigating this problem numerically to understand how such an instability can be triggered by a simple A+B-->C reaction when a solution of reactant A is displacing linearly a miscible solution of B of same viscosity producing a more viscous product C at the interface. The properties of the fingering patterns observed in the zone where less viscous A pushes more viscous C have been shown to vary with the speed of reaction, the viscosity contrast between reactants and product, the ratio of initial concentrations of A and B and the diffusion coefficients of each species. In particular our study shows that the fingering pattern is different whether A displaces B or vice-versa as soon as the reactant species have different diffusion coefficients or are injected with a different concentration. This result is enlightening recent experimental observations of such asymmetries in radial fingering of micellar systems [34].

To gain experimental insight into such reaction-driven viscous fingering, we are currently developing an experimental study in a linear displacement inside a horizontal Hele-Shaw cell of the system initially studied in a radial injection by Podgorski et al. [34]. The reactant A and B solutions are aqueous solutions of a cationic surfactant (cetyltrimethylammonium bromide - CTAB) and of salicylic acid (NaSal) respectively. They form upon contact a highly viscous gel-like micellar system. Viscous fingering occurs therefore in this reactive system as soon as one of the reactant solution is injected into the other one because at their interface more viscous product is synthesized (Fig.9).

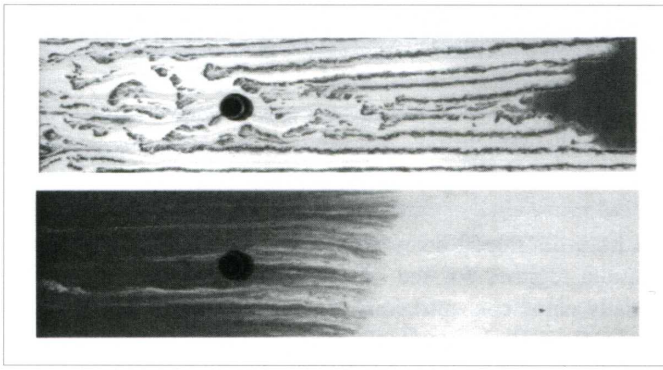

Fig.9 : Viscous fingering of a reactive interface developing when an aqueous solution of 50 mM CTAB is displacing linearly from left to right in a Hele-Shaw cell a solution of 50 mM NaSal colored in black (top) or vice-versa (bottom) at an injection speed of 2.5 mm/s. The dark circle is the inlet for radial displacement (not used here).

The main interest of this system is that it is an archetype for a truly reaction-driven hydrodynamic instability. Indeed, as the two reactant solutions both have the viscosity of water, no viscous fingering instability would be expected a priori. It is only thanks to the reaction which is modifying the viscosity that fingering can occur. Interestingly (and as already observed previously in a radial injection by Podgorski et al. [34]), linear displacement gives striking different fingering patterns whether A displaces B or vice-versa in this micellar system (Fig.9). More theoretical and experimental work is currently underway to unravel the properties of such reaction-driven fingering.

7. Conclusions

The variety of spatio-temporal dynamics resulting from the coupling between chemical reactions and diffusive processes has long been the subject of numerous studies. If, in addition, hydrodynamic motions come into play, the situation can often become quite complex. Of particular interest to us among the wealth of possible situations involving the coupling between reactions and diffusive or convective transport processes are

situations where the chemical reaction is itself at the very source of hydrodynamic instabilities as it provides not only the interface to become hydrodynamically unstable but also the gradients in density, surface tension or viscosity that create the fluid flow. We have summarized here the research performed (mainly from a theoretical perspective but more recently also from an experimental view) in our group in this context and that aims at contributing to the prediction and characterization of new chemo-hydrodynamic patterns and instabilities.

Acknowledgements

I thank all past and present members and visitors of the Nonlinear Physical Chemistry Unit of ULB whose research results have been detailed here for their fruitful collaboration. I acknowledge financial support from FRS-FNRS, Prodex, ESA and the Communauté française de Belgique (ARC-Archimedes programme).

1 G. Nicolis and I. Prigogine, *Self-organization in nonequilibrium systems* (Wiley, New York, 1977) ; R. Kapral and K. Showalter Eds, *Chemical waves and patterns* (Kluwer Academic Publisher, 1994).
2 I.R. Epstein and J.A. Pojman, *An introduction to nonlinear chemical dynamics* (Oxford University Press, Oxford, 1988).
3 A. De Wit, *Adv. Chem. Phys.* **1999**, *109*, 435.
4 J. Fernandez, P. Kurowski, P. Petitjeans and E. Meiburg, *J. Fluid Mech.*, **2002**, *451*, 239.
5 A.A. Nepomnyashchy, M.G. Velarde and P. Colinet, *Interfacial phenomena and convection* (Chapman and Hall, London/ CRC, Boca Raton, 2002).
6 G.M. Homsy, *Ann. Rev. Fluid Mech.*, **1987**, *19*, 271.
7 J.A. Pojman and I. R. Epstein, *J. Phys. Chem.*, **1990**, *94*, 4966.
8 A. De Wit, *Phys. Rev. Lett.*, **2001**, *87*, 054502.
9 J. D'Hernoncourt, A. Zebib and A. De Wit, *Chaos*, **2007**, *17*, 013109.
10 J. D'Hernoncourt, A. Zebib and A. De Wit, *Phys. Rev. Lett.*, **2006**, *96*, 154501.
11 M. Böckmann and S. C. Müller, *Phys. Rev. Lett.*, **2000**, *85*, 2506.
12 D. Horváth, T. Bánsági Jr., and A. Tóth, *J. Chem. Phys.* **2002**, *117*, 4399.
13 J. Yang, A. D'Onofrio, S. Kalliadasis and A. De Wit, *J. Chem. Phys.*, **2002**, *117*, 9395.
14 A. De Wit, *Phys. Fluids*, **2004**, *16*, 163.
15 J. D'Hernoncourt, S. Kalliadasis and A. De Wit, *J. Chem. Phys.*, **2005**, *123*, 234503.
16 T. Bánsági Jr., D. Horváth, A. Tóth, J. Yang, S. Kalliadasis and A. De Wit, *Phys. Rev. E*, **2003**, *68*, 055301(R).
17 L. Rongy, N. Goyal, E. Meiburg and A. De Wit, *J. Chem. Phys.*, **2007**, 127, 114710.
18 L. Pismen, *Phys. Rev. Lett.*, **1997**, *78*, 382.
19 L. Rongy and A. De Wit, *J. Chem. Phys.*, **2006**, *124*, 164705.
20 L. Rongy and A. De Wit, *J. Eng. Math.*, **2007**, *59*, 221.
21 L. Rongy and A. De Wit, *Phys. Rev. E*, **2008**, *77*, 046310.
22 L. Galfi and R. Racz, *Phys. Rev A*, **1988**, *38*, 3151.
23 Y.-E. L. Koo and R. Kopelman, *J. Stat. Phys.*, **1991**, *65*, 893.
24 Y. Shi and K. Eckert, *Chem. Eng. Sci.*, **2006**, *61*, 5523.
25 L. Rongy, P.M.J. Trevelyan and A. De Wit, *Phys. Rev. Lett.*, **2008**, *101*, 084503.
26 G.G. Casado, L. Tofaletti, D. Müller and A. D'Onofrio, *J. Chem. Phys.*, **2007**, *126*, 114502.
27 J.S. Turner, *Buoyancy effects in fluids* (Cambridge University Press, 1973).
28 L.D. Plante, P.M. Romano and E.J. Fernandez, *Chem. Eng. Sci.*, **1994**, *49*, 229.
29 B.S. Broyles, R.A. Shalliker, D.E. Cherrak and G. Guiochon, *J. Chromatogr. A*, **1998**, *822*, 173.
30 A. De Wit, Y. Bertho and M. Martin, *Phys. Fluids*, **2005**, *17*, 054114.
31 G. Rousseaux, A. De Wit and M. Martin, *J. Chromatography A* , **2007**, *1149*, 254.
32 M. Mishra, M. Martin and A. De Wit, *Phys. Fluids*, **2007**, *19*, 073101.
33 Y. Nagatsu, K. Matsuda, Y. Kato and Y. Tada, *J. Fluid Mech.*, **2007**, *571*, 475.
34 T. Podgorski, M.C. Sostarecz, S. Zorman, and A. Belmonte, *Phys. Rev. E*, **2007**, *76*, 016202.